

User-defined quantum key distribution

Zhengyu Li^{1,2†}, Yichen Zhang^{3†}, and Hong Guo^{1*}

¹*State Key Laboratory of Advanced Optical Communication Systems and Networks,
School of Electronics Engineering and Computer Science, Center for Quantum Information Technology,
Center for Computational Science and Engineering, Peking University, Beijing 100871, China*

²*Central Research Institute, 2012 Labs, Huawei Technologies Co., Ltd, Shenzhen, Guangdong, China*

³*State Key Laboratory of Information Photonics and Optical Communications,
Beijing University of Posts and Telecommunications, Beijing 100876, China and*

[†]*These authors contribute equally to this work.*

(Dated: May 14, 2018)

Quantum key distribution (QKD) provides secure keys resistant to code-breaking quantum computers. As headed towards commercial application, it is crucial to guarantee the practical security of QKD systems. However, the difficulty of security proof limits the flexibility of protocol proposals, which may not fulfill with real application requirements. Here we show a protocol design framework that allows one to securely construct the protocol using arbitrary non-orthogonal states. Multi-mode entangled source is virtually introduced for the security analysis, while coherent measurement is used to provide raw data. This ‘arbitrary’ feature reverses the traditional protocol-decide-the-system working style, such that the protocol design now can follow what the system generates. We show a valuable showcase, which not only solves the security challenge of discrete-modulated coherent states, but also achieves high performance with no more than 256 coherent states. Our findings lower the requirement for system vendors with off-the-shell devices, thus will promote the commercialization of QKD.

PACS numbers: 03.67.Dd, 03.67.Hk

BB84 protocol [1] started the era of quantum cryptography, among which quantum key distribution (QKD) [2–4] is the most applicable technology, providing physical-layer protection of information transmission through secure distribution of private keys. For cost-effective implementation, a practical system usually carries out the prepare-and-measure (PM) scheme of a QKD protocol, in which non-orthogonal states are randomly prepared by Alice (the sender), and transmitted to Bob (the receiver), who will measure the states with either single-photon detection or coherent measurement (homodyne or heterodyne detection) [5–8]. Systems with coherent detectors are more attractive to commercial companies, due to its room-temperature operation feature and the compatibility with mature product chain of telecommunication. Protocols with coherent measurement usually encode key information on quadratures of a quantum optical state, which are usually called continuous variable (CV) protocols [9–11].

The most influential CV protocol is GG02 protocol using Gaussian modulated coherent states [6, 12]. It later evolves to various Gaussian protocols [7, 8, 13] with theoretical security proof [14–18], outperforming other CV protocols. To maintain the practical security [3] of a protocol running in a system, the system should fulfill the theoretical assumptions in security proof. However, even the most state-of-the-art components cannot remove all the theory-experiment mismatches, for instance, the continuous modulation of Gaussian protocols can never be achieved with finite resolution digital-to-analog-converter (DAC) [19]. These mismatches also are one of the motivations for the exploration of CV protocols using discrete modulation [20–22], but their performances are not promis-

ing as Gaussian protocols. Therefore, it’s desired for such a protocol that it is adjustable according to practical systems.

Here we move one step forward, proposing a new CV protocol design framework, which allows one to construct the protocol using arbitrary non-orthogonal states with rigorous security analysis. Numerous protocols can be proposed by choosing different non-orthogonal states, which can be discretely or continuously distributed, and can be pure or mixed. This ‘arbitrary’ feature makes the protocol design can be customized by any system vendor according to what they can actually manufacture.

The framework contains two duel schemes, one is the PM scheme, and the other is the entanglement-based (EB) scheme [23], which is the core design of our framework. The main idea is that Alice uses multi-mode entangled state as the source, and conducts positive-operator valued measures (POVMs) and coherent measurements on different modes. The results of POVMs correspond to the key information in Alice’s side, and decide which state is sent out. The results of coherent measurements are used to estimate the correlation between Alice and Bob, through which the lower bound of the secret key rate can be calculated.

Let us explain our framework using schematics in Fig. 1. Due to finite resolution of devices, discrete modulation is always the case in practical applications, therefore we describe our framework in discrete form. The PM scheme of our framework is quite similar as a general QKD protocol. There are n (≥ 2) different non-orthogonal states $\{\rho_{B_0}^1, \rho_{B_0}^2, \dots, \rho_{B_0}^n\}$ that Alice could possibly send to Bob with non-zero probabilities $\{p_1, p_2, \dots, p_n\}$. For each time, which state will be sent is decided by the first random number (a complex number or a vector) generated by a quantum random number generator (QRNG). Bob measures the received state ρ_B with coherent measurement, and then they do the post-processing [24, 25]. The dif-

* Corresponding author: hongguo@pku.edu.cn

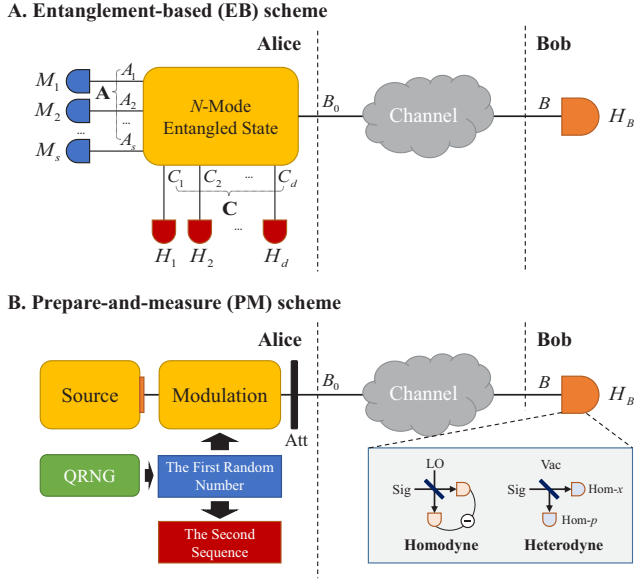


FIG. 1. **Schematics for EB and PM schemes of our framework.** (A) EB scheme. The entangled source is an N -mode state, among which there are $s (\geq 1)$ modes $A_1 A_2 \dots A_s$ measured by some POVMs, and other $d (\geq 1)$ modes $C_1 C_2 \dots C_d$ will be measured by heterodyne detectors. Mode B_0 is sent to Bob. (B) PM scheme. The state generation is accomplished by modulating the light source, followed with a strong attenuation. The modulation is controlled by the first random number (or a random vector) which can be acquired through a QRNG. The second sequence is decided by the first random number. Bob's measurement can be either homodyne (Hom) or heterodyne (Het) detection. Att: Attenuator. LO: Local oscillator. Vac: Vacuum. Hom- $x(p)$: homodyne detection for $x(p)$ quadrature.

ference is, Alice additionally needs a second sequence for the security analysis (see explanation later).

The equivalence of the EB scheme lies in the design of Alice's entangled source and measurements. The entangled source $|\psi_{ACB_0}\rangle$ is an N -mode purification of the mixed state $\rho_{B_0} = \sum_{i=1}^n p_i \rho_{B_0}^i$, in which the subscript A represents s modes $A_1 A_2 \dots A_s$, C represents d modes $C_1 C_2 \dots C_d$, and $s + d + 1 = N$, $s \geq 1$, $d \geq 1$. Alice keeps modes A and C , while sends mode B_0 to Bob. The measurements for modes A are POVMs, with the results recorded as $M_A = (m_1, m_2, \dots, m_s)$; and the measurements for modes C are heterodyne measurements, with the results recorded as $H_C = (h_1, h_2, \dots, h_d)$. We require that these measurements will project mode B_0 onto a state $\rho_{B_0}^{M_A, H_C} \in \{\rho_{B_0}^1, \rho_{B_0}^2, \dots, \rho_{B_0}^n\}$. After sending the state $\rho_{B_0}^{M_A, H_C}$ to Bob, the rest are the same as the PM scheme.

To show the validity of our framework for arbitrary non-orthogonal states, we first give a sufficient condition to find such an N -mode purification. It is that which state is sent to Bob is only decided by the POVMs results M_A . This means the sub-state of modes C and B_0 conditioned on the results M_A is a product state, $\rho_{CB_0}^{M_A} = \rho_C^{M_A} \otimes \rho_{B_0}^{M_A}$. Then among the purifications of such mixed state $\rho_{CB_0} = \sum_{i=1}^n p_i \rho_C^i \otimes \rho_{B_0}^i$, the entangled source $|\psi_{ACB_0}\rangle$ and the corresponding POVMs for modes A can always be found. This sub-state product feature

is also the necessary condition if the non-orthogonal states are coherent states.

Second, we explain how to calculate the secret key rate. Here we restrict to the reverse reconciliation and asymptotic case [12, 26], which is the base for other cases. The key part is to evaluate the Holevo information [27] $S(H_B : E)$ between Bob's data and the quantum adversary, whose upper bound S_{BE}^G can be got through the covariance matrix γ_{ACB} thanks to the Gaussian state extremality theorem [15, 28]. However, the POVMs for modes A make γ_{ACB} incomplete. More specifically, if γ_{ACB} is expressed in the form of several sub-matrices,

$$\gamma_{ACB} = \begin{pmatrix} \gamma_A & \phi_{AC} & \kappa_{AB} \\ \phi_{AC}^T & \gamma_C & \phi_{CB} \\ \kappa_{AB}^T & \phi_{CB}^T & \gamma_B \end{pmatrix} \quad (1)$$

then the covariance term κ_{AB} is unknown. For other terms, γ_A , γ_C , and ϕ_{AC} can be theoretically calculated, and ϕ_{CB} , γ_B can be estimated through the measured data. Now S_{BE}^G becomes a function of an unknown variable κ_{AB} . Nevertheless, the uncertainty principle puts a constraint on the covariance matrix of a physical state [10], which limits the possible value of κ_{AB} to a set S_κ . If we denote ϕ_{AB}^{Eve} as the real eavesdropping induced κ_{AB} , then $\phi_{AB}^{Eve} \in S_\kappa$. Therefore, by finding the maximum $S_{BE}^G(\kappa_{AB})$ through traversing the set S_κ , we can define the secret key rate as

$$K_R = \beta I(M_A : H_B) - \sup_{\kappa_{AB} \in S_\kappa} S_{BE}^G(\kappa_{AB}), \quad (2)$$

where $I(M_A : H_B)$ is the classical mutual information, and β is the reconciliation efficiency.

Now we can explain what the second sequence in the PM scheme is. Originally, it should be the measurements results H_C , which can be simulated by a QRNG since all modes C are kept in Alice's side. If further exploiting the product feature of $\rho_{CB_0}^{M_A}$, the estimation of ϕ_{CB} requires only the mean values of quadratures for the sub-state $\rho_C^{M_A}$. Then a simpler form of the second sequence is $\{\bar{x}_{C_1}^{M_A}, \bar{p}_{C_1}^{M_A}, \dots, \bar{x}_{C_d}^{M_A}, \bar{p}_{C_d}^{M_A}\}$, where $\bar{x}_{C_i}^{M_A} = \text{Tr}_C(\hat{x}_{C_i} \rho_C^{M_A})$, and $\bar{p}_{C_i}^{M_A} = \text{Tr}_C(\hat{p}_{C_i} \rho_C^{M_A})$. This simple form can

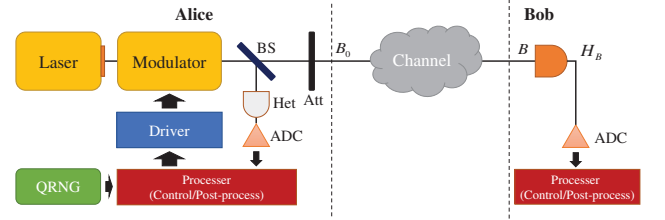


FIG. 2. **State preparation calibration.** In a coherent-state system, to check what state is really generated, a beamsplitter (BS) is inserted between the modulator and the attenuator. One output of the BS will be measured by a heterodyne detector (Het). The measurement result will be sampled and sent to the processor (used for system control and post-processing), in which the relationship between the data and the modulation result is processed. ADC: Analog-to-Digital Converter.

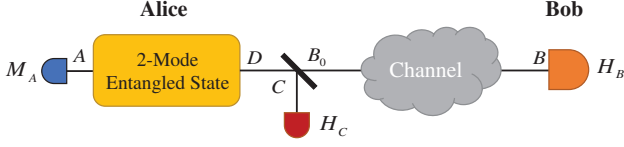


FIG. 3. **The specific three-mode protocol for coherent states.** The three-mode entangled source is acquired through a two-mode entangled state $|\psi_{AD}\rangle$. Mode D interacts with the vacuum on a beamsplitter, then the two output modes are C and B_0 .

be realized digitally in the processor, since it's decided by the first random number, not independently random. Therefore, the PM scheme has no change in hardware comparing to the existing CV-QKD system.

System vendors, as the direct user of protocols, used to build the system following the instruction of a protocol. Now in contrast to this tradition, the protocol can be customized following a practical system. A vendor can start with checking what states their system can generate, then set the probability of sending each state. For the rest, one can follow our framework to find a proper N -mode purification, and the secret key rate formula can be got.

Protocols using coherent states are usually the choice of vendors due to the low-cost laser source. The state is generated by modulating the laser with an intensity modulator (IM) and a phase modulator (PM) or a quadrature-phase shift keying (QPSK) modulator, followed by a strong attenuation. Such modulation using off-the-shell devices usually suffers problems as discretization, non-linearity and noise. To check what the state is actually generated, one can use an additional measurement structure, shown in Fig. 2. The modulated light passes a beamsplitter before entering the attenuator, and a large portion of it goes to a heterodyne detector. Then the modulation result can be read-out with high signal-to-noise ratio (SNR), since the noise figure of classical detectors performs well in the bandwidth of a QKD system (usually less than 1GHz). This step can be a pre-calibration procedure, or a continuous feedback during the whole running time. Once the map between Alice's data and its real modulation result is set up, it can also be used to compensate the modulation error. Only small deviation remains.

We found an effective way to build the EB scheme for the case using coherent states. We choose three-mode entangled source $|\psi_{ACB_0}\rangle$ for simplicity, and our design principle is to maximize the correlation between modes C and B_0 , which can limit the eavesdropper. This leads to the choice for each ρ_C^i that it's also a coherent state $|\alpha_C^i\rangle$ with the mean value linearly dependent on $|\alpha_{B_0}^i\rangle$. Following this way, one only needs to find a two-mode entangled state $|\psi_{AD}\rangle$, then mode D passing a beamsplitter will result in the $|\psi_{ACB_0}\rangle$, as shown in Fig. 3.

To achieve the same high performance as ideal Gaussian protocols, our framework can reduce the necessary number of used coherent states to no more than 256. Comparing to generating around 1 million coherent states in Gaussian protocols, requested to suppress the theory-experiment mismatch [19], this will greatly reduce the complexity of state

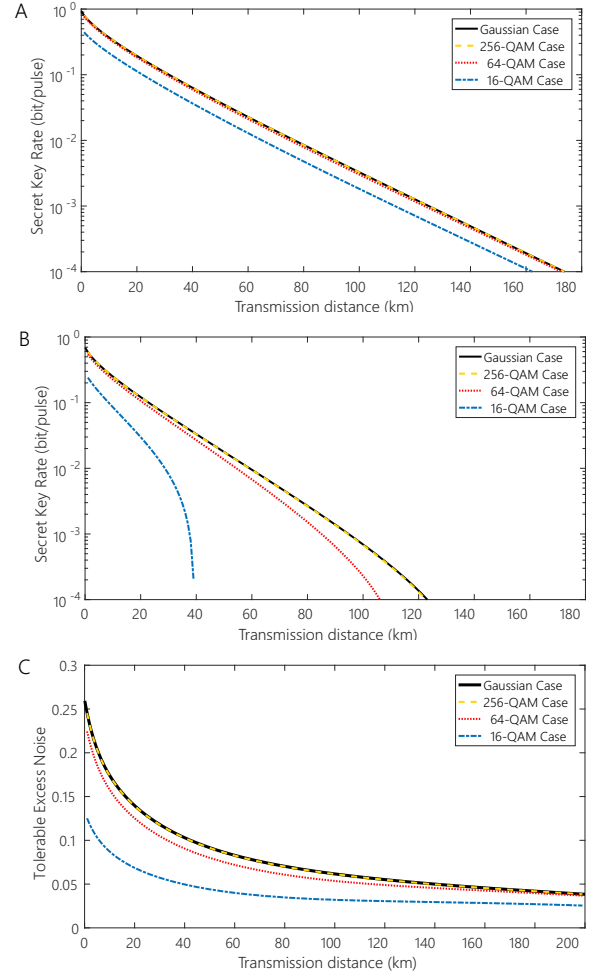


FIG. 4. **Secret key rates and tolerable excess noises.** (A) Secret key rate for low channel noise case ($\epsilon_C = 0.01$). (B) Secret key rate for high channel noise case ($\epsilon_C = 0.05$). (C) Tolerable excess noise. The black solid line represents the ideal Gaussian case, the blue dash-dotted line represents 16-QAM case, the red dotted line represents 64-QAM case, the yellow dashed line represents 256-QAM case. Simulation details are explained in the supplementary information.

preparation. Now only 4-bits resolution for each quadrature's modulation is required, which means the modulation noise is negligible, considering the fact that the equivalent-number-of-bit (ENOB) for an off-the-shell DAC can usually reach higher than 10 bits. Different constellation of $|\alpha_{B_0}^i\rangle$ will influence the protocol's performance. We show some performance simulations of standard quadrature-amplitude-modulation (QAM) with different number of states in Fig. 4, which is commonly used constellation in classical telecommunication. One can find that with proper settings, 256-QAM can reach the performance almost the same as ideal Gaussian case. And for the low noise case, the number of coherent states can be further reduced to 64, or even lower as 16 for short range. Small-deviation non-standard QAMs, which may happen due to the uncompensated modulation non-linearity, have the similar performances.

Other constellation maps can also be introduced, and run on the same hardware. The switch among pre-set or freshly user-defined constellation maps can be actively controlled by customers, through software-defined manner. This complies the trend of telecommunication network. Combined with the simple modulation and allowance for using off-the-shell devices, our framework will promote the commercialization of QKD.

We thank C. Su, L. Lu, Y. Zou, Y. Cai and B. Xu for discussions. This work was supported by the National Natural Science Foundation under Grant 61531003.

APPENDIX A: SECRET KEY RATE

Here we explain our derivation of the secret key rate formula. The state-of-the-art security analysis method is deriving the secret key length formula in the finite-size regime under the universal composable framework (UCF) [16–18]. First, one needs to reduce the full formula (quantized by the smooth min-entropy) to a lower bound, which usually is the asymptotic secret key rate with modification terms related to the block size. Then derive a lower bound of the asymptotic secret key rate, which should be calculable through only the measured data. The first reduction relies on several theoretical theorems, differing for different entangled states and measurements used in the protocol, and this is an open question for our framework. Therefore, here we focus on the asymptotic secret key rate formula, and discuss the reverse reconciliation case.

A generally used secret key rate for the asymptotic case is the Devetak-Winter formula [26],

$$K = \beta I(M_A : H_B) - S(H_B : E), \quad (3)$$

where $I(M_A : H_B)$ is the classical mutual information between Alice and Bob, β is the classical reconciliation efficiency, and $S(H_B : E)$ is the Holevo information between Bob's data and the adversary [27]. Usually, $S(H_B : E)$ can be replaced by any of its upper bounds $\bar{S}(H_B : E)$, among which the Gaussian state extrametry theorem [15, 28] induced upper bound S_{BE}^G is the most commonly used case. Because its calculation only relies on the covariance matrix γ_{ACB} , which can be estimated through the experimental data.

The covariance matrix γ of a N -mode state $\hat{\rho}_N$ is defined as [10],

$$\gamma_{ij} := \frac{1}{2} \langle \{\Delta \hat{r}_i, \Delta \hat{r}_j\} \rangle, \quad (4)$$

where $\hat{\mathbf{r}} = \{\hat{x}_1, \hat{p}_1, \dots, \hat{x}_N, \hat{p}_N\}$, $\langle \hat{r}_i \rangle = \text{Tr}(\hat{r}_i \hat{\rho}_N)$, and $\Delta \hat{r}_i = \hat{r}_i - \langle \hat{r}_i \rangle$. Suppose γ_{ACB} is the covariance matrix of the state ρ_{ACB} , which is the state after mode B_0 of the entangled source $|\psi_{ACB_0}\rangle$ arriving at Bob's side through the channel. It can be represented using several sub-matrices,

$$\gamma_{ACB} = \begin{pmatrix} \gamma_A & \phi_{AC} & \kappa_{AB} \\ \phi_{AC}^T & \gamma_C & \phi_{CB} \\ \kappa_{AB}^T & \phi_{CB}^T & \gamma_B \end{pmatrix} \quad (5)$$

where γ_A , γ_C and γ_B are covariance matrices for modes **A**, **C** and **B**, and ϕ_{AC} , ϕ_{CB} and κ_{AB} are covariance terms between different modes.

Among all these sub-matrices, γ_A , γ_C and ϕ_{AC} can be directly calculated from $|\psi_{ACB_0}\rangle$, since modes **A** and **C** are kept in Alice's side. ϕ_{CB} and γ_B can be estimated after Alice and Bob randomly sharing part of their coherent measurement results. The only unknown sub-matrix is κ_{AB} , since the measurements for modes **A** are not coherent measurements now.

Nevertheless, the covariance matrix γ_N for a N -mode state is constrained by the uncertainty principle [10], which is

$$\gamma_N + i\Omega_N \geq 0, \quad (6)$$

where $\Omega_N = \text{diag}(\omega_1, \omega_2, \dots, \omega_N)$, and

$$\omega_1 = \dots = \omega_N = \omega = \begin{pmatrix} 0 & 1 \\ -1 & 0 \end{pmatrix}. \quad (7)$$

We denote S_κ^ψ as the set of all κ_{AB} satisfying this constraint for γ_{ACB} , which is

$$S_\kappa^\psi = \{\phi_{AB} | \gamma_{ACB} [\kappa_{AB} = \phi_{AB}] + i\Omega_N \geq 0\}. \quad (8)$$

If ϕ_{AB}^{Eve} is the real eavesdropping induced κ_{AB} , then $\phi_{AB}^{Eve} \in S_\kappa^\psi$. It can be understood that S_{BE}^G is a function of κ_{AB} now. Then by traversing the set S_κ^ψ for all possible κ_{AB} , we can find the maximum of S_{BE}^G . Then the secret key rate can be wrote as

$$K_R = \beta I(M_A : H_B) - \sup_{\kappa_{AB} \in S_\kappa^\psi} S_{BE}^G(\kappa_{AB}). \quad (9)$$

Next we briefly introduce the calculation method for each term. For $\beta I(M_A : H_B)$, it can be expressed as $\beta I(M_A : H_B) = H(H_B) - \text{leak}_{EC}$, in which $H(H_B)$ is the Shannon entropy of Bob's measurement results, and leak_{EC} represents the information that Bob sends to Alice for the data reconciliation. Both these terms can be got from measured data and the error correction step. The reason that we usually separate $\beta I(M_A : H_B)$ into β and $I(M_A : H_B)$ in theoretical study is this helps numerical simulation, which is used to evaluate the performance of a protocol. Given the channel model (usually required to fit the experimental environment), the probability $p(H_B|i)$ can be got from the model, which is the probability of getting Bob's measurement result H_B given Alice sending the state $\rho_{B_0}^i$. And the overall probability will be $p(H_B) = \sum_{i=1}^n p_i p(H_B|i)$. If H_B is a discrete variable quantized from the measurement result, then

$$\begin{aligned} I(M_A : H_B) &= - \sum_{H_B} p(H_B) \log_2 p(H_B) + \sum_{i=1}^n p_i \sum_{H_B} p(H_B|i) \log_2 p(H_B|i). \end{aligned} \quad (10)$$

If consider H_B as the continuous variable for some theoretical research, the sum of H_B will be replaced by integration. The reconciliation efficiency β can be set according to certain error correction code, for instance, 0.95 is achievable for multi-dimensional reconciliation method in low signal-to-noise regime [29].

For $\sup_{\kappa_{AB} \in S_\kappa^\psi} S_{BE}^G(\kappa_{AB})$, we traverse each $\kappa_{AB} \in S_\kappa^\psi$ to calculate its corresponding $S_{BE}^G(\kappa_{AB})$ and find the maximal value of them. $S_{BE}^G(\kappa_{AB})$ can be expressed as $S(\rho_{ACB}^G|\kappa_{AB}) - S(\rho_{AC|B}^G|\kappa_{AB})$, in which $S(\rho_{ACB}^G|\kappa_{AB})$ means the von Neumann entropy of a Gaussian state ρ_{ACB}^G which has the same covariance matrix as $\gamma_{ACB}(\kappa_{AB})$, and $S(\rho_{AC|B}^G|\kappa_{AB})$ means the von Neumann entropy of a conditional Gaussian state $\rho_{AC|H_B}^G$ which has the same covariance matrix as $\gamma_{AC|H_B}$, related to Bob's measurement method. The methods to get the $\gamma_{AC|H_B}$ from γ_{ACB} , to get the symplectic eigenvalues of each covariance matrix, and to calculate the von Neumann entropy are commonly used in CV-QKD, and can be found in reference [10, 15].

APPENDIX B: THE SIMPLE FORM OF THE SECOND SEQUENCE

In the covariance matrix γ_{ACB} , γ_A , γ_C and ϕ_{AC} can be theoretically calculated, and γ_B is estimated only using Bob's data. Only the estimation of ϕ_{CB} will use the measurement results of modes C. Naturally, the second sequence should be the measurement results H_C for modes C, which can be simulated through a quantum random number generator (QRNG). However, the product feature of sub-state $\rho_{CB_0}^i$ can help to simplify this.

Let's take the x -quadrature of mode C_1 as an example. After tracing out the other modes of C, the state of modes C_1 and B_0 is $\rho_{C_1 B_0} = \sum_{i=1}^n p_i \rho_{C_1}^i \otimes \rho_{B_0}^i$, where $\rho_{C_1}^i = \text{Tr}_{C_2 \dots C_s}(\rho_C^i)$. Then

$$\begin{aligned} \langle \Delta \hat{x}_{C_1} \Delta \hat{x}_{B_0} \rangle &= \sum_{i=1}^n p_i \text{Tr}_{C_1 B_0} [(\hat{x}_{C_1} - \bar{x}_{C_1})(\hat{x}_{B_0} - \bar{x}_{B_0}) \rho_{C_1}^i \otimes \rho_{B_0}^i] \\ &= \sum_{i=1}^n p_i (\bar{x}_{C_1}^i - \bar{x}_{C_1})(\bar{x}_{B_0}^i - \bar{x}_{B_0}), \end{aligned} \quad (11)$$

in which each $\bar{x}_{C_1}^i = \text{Tr}_{C_1}(\hat{x}_{C_1} \rho_{C_1}^i)$ and $\bar{x}_{C_1} = \sum_{i=1}^n p_i \bar{x}_{C_1}^i$ can be theoretically calculated. Therefore, if the first random number decides that $\rho_{B_0}^i$ will be sent, then it's enough to let the second sequence be $\{\bar{x}_{C_1}^i, \bar{p}_{C_1}^i, \dots, \bar{x}_{C_d}^i, \bar{p}_{C_d}^i\}$ for the calculation of ϕ_{CB} . This is much simpler than simulating the heterodyne results H_C using quantum random numbers.

APPENDIX C: THE PRODUCT FEATURE OF SUB-STATE $\rho_{CB_0}^{M_A}$ IS NECESSARY

The EB scheme plays the key role in our framework, in which we need to find a proper entangled source and the measurements in Alice's side. Here we explain one detail of our design solution. Consider the case that one wants to use finite discrete-distributed coherent states as the non-orthogonal source, which is the most significant case for practical implementation. In this case, it is necessary to require that the sub-state $\rho_{CB_0}^{M_A}$ of modes C and B_0 conditioned on the POVMs results M_A is a product state.

To explain this necessity, we first prove a lemma which is

Lemma 1. For any two-mode entangled state ρ_{AB} , if after the heterodyne detection over mode A, mode B is projected onto a coherent state, then the number of possibly projected coherent states for mode B is either one or infinite.

We prove this by contradiction. Suppose ρ_{AB} satisfies that mode B is a coherent state after the heterodyne detection over mode A, and the number n of the possibly projected coherent state is $\infty > n \geq 2$.

For generality, we assume ρ_{AB} is a mixed state. There exists a purification of ρ_{AB} , which can be expressed as $\rho_{FAB} = \sum_{i=1}^n \sqrt{p_i} |\phi_{FA}^i\rangle |\alpha_B^i\rangle$. The heterodyne detection can be seen as the projection onto a coherent state $|\alpha_A\rangle$. We divide the overall phase space for mode A into $n+1$ different sets $\{\zeta_1, \zeta_2, \dots, \zeta_{n+1}\}$, among which any two of them has no overlap. This equals to divide the two-dimensional plane into $n+1$ points sets without overlap. The first n sets correspond to the n different output coherent states of mode B. For example, for the heterodyne measurement result α_A , if $\alpha_A \in \zeta_i$, then mode B will be projected onto $|\alpha_B^i\rangle$. And we assume for each element of the first n sets, the probability of getting a corresponding heterodyne result for mode A is non-zero. The last set ζ_{n+1} corresponds to the points that will never be the heterodyne result, which means $\text{Tr}_B[\langle \alpha_A | \rho_{AB} | \alpha_A \rangle] = 0$, if $\alpha_A \in \zeta_{n+1}$.

Suppose $1 \leq k \leq n$, and $\alpha_A \in \zeta_k$, then we know

$$|\alpha_B^k\rangle \langle \alpha_B^k| = \sum_{i,j=1}^n C_{ij} |\alpha_B^i\rangle \langle \alpha_B^j|, \quad (12)$$

where $C_{ij} = (\sqrt{p_i p_j} / p(\alpha_A)) \cdot \text{Tr}_F[|\alpha_A\rangle \langle \alpha_A| |\phi_{FA}^i\rangle \langle \phi_{FA}^j|]$, and $p(\alpha_A)$ is the probability of getting the measurement result α_A .

First, we can prove that if $i \neq k$ or $j \neq k$, then $C_{ij} = 0$, which means the only non-zero term is $C_{kk} = 1$. The intuitive understanding of this is that, there are infinite equations constraining finite variables C_{ij} . The detailed proof can follow these steps:

1) derive $D(-\alpha_B^k) |\alpha_B^k\rangle \langle \alpha_B^k| D^\dagger(-\alpha_B^k)$, and move the vacuum state term to one side,

$$(1 - C_{kk}) |0\rangle \langle 0| = \sum_{i,j=1, i,j \neq kk}^n C_{ij} |\alpha_B^i - \alpha_B^k\rangle \langle \alpha_B^j - \alpha_B^k|. \quad (13)$$

2) calculate the inner product between the Fock state $|t\rangle$ and the vacuum state,

$$0 = \sum_{i,j=1, i,j \neq kk}^n C_{ij} e^{-|\beta_i|^2/2} e^{-|\beta_j|^2/2} \beta_i^t \beta_j^{*t} / t!, \quad \forall t \geq 1, \quad (14)$$

where $\beta_i = \alpha_B^i - \alpha_B^k, \beta_j = \alpha_B^j - \alpha_B^k$.

If let $\lambda_{ij} = \beta_i \beta_j^*, d_{ij} = C_{ij} \exp[-(|\beta_i|^2 + |\beta_j|^2)/2]$, then the first $n^2 - 1$ equations can be written in the matrix formula $\Lambda \mathbf{D} = 0$, in which Λ is the transport of a Vandermonde matrix with $n^2 - 1$ different non-zero λ_{ij} , and \mathbf{D} is a vector with $n^2 - 1$ different d_{ij} . Since the Vandermonde matrix has the feature of full rank, then the above equations have the only solution that each $d_{ij} = 0$, which means $\forall i, j \neq kk, C_{ij} = 0$, and $C_{kk} = 1$.

Second, for any $\varsigma_k, 1 \leq k \leq n+1$, we can define a corresponding set τ_k of coherent states, which is $\tau_k = \{|\alpha_A\rangle \mid \alpha_A \in \varsigma_k\}$. Then the above discussion will lead to the conclusion that, for each τ_k , there exists at least one state orthogonal to it. First look at the case $1 \leq k \leq n$, in which $C_{ii} = 0$ for any $i = j \neq k$. This means $\forall |\alpha_A\rangle \in \tau_k, \langle \alpha_A | \rho_A^{ii} | \alpha_A \rangle = 0$, where $\rho_A^{ii} = \text{Tr}_F [|\phi_{FA}^i\rangle\langle\phi_{FA}^i|]$. Then ρ_A^{ii} is orthogonal to the set τ_k . Second, for the case $k = n+1$, from its definition we know $\text{Tr}_B [\langle \alpha_A | \rho_{AB} | \alpha_A \rangle] = 0$, if $|\alpha_A\rangle \in \varsigma_{n+1}$. Then $\rho_A = \text{Tr}_B [\rho_{AB}]$ is orthogonal to τ_{n+1} .

However, it can be proved that when n is finite, among all these $n+1$ set $\{\tau_1, \tau_2, \dots, \tau_{n+1}\}$, at least there is one of them being a complete or over-complete set of the Fock state space [30], which means no state can be orthogonal to this set. This is contradictory to the previous conclusion. Therefore, for the case $\infty > n \geq 2$, no such a two-mode entangled state can be found. \square

One can easily generalize this to the N -mode entangled state case, which is, for any N -mode entangled state ρ_{AB} , if after the heterodyne detections for each mode of **A**, mode **B** is projected onto a coherent state, then the number of possibly projected coherent states for mode **B** is either one or infinite.

For our EB scheme, after the POVMs for modes **A**, the conditioned sub-state $\rho_{CB_0}^{M_A}$ will face the same situation as the above argument. And what we consider is the finite coherent states case, then the number of possibly projected coherent states for mode B_0 is only one. This means $\rho_{CB_0}^{M_A}$ is a product state that $\rho_{CB_0}^{M_A} = \rho_C^{M_A} \otimes |\alpha_{B_0}^{M_A}\rangle\langle\alpha_{B_0}^{M_A}|$.

The above conclusion shows four facts about our framework: 1) POVM measurements other than heterodyne detection should be introduced; 2) entangled state with more than two modes are necessary; 3) after the POVMs, the conditioned sub-state should be a product state; 4) which coherent state will be sent to Bob is decided by the results of POVMs.

APPENDIX D: THREE-MODE PROTOCOL FOR FINITE DISCRETE-DISTRIBUTED COHERENT STATES

For a CV system, generating discrete-distributed coherent states is the most practical case, because of the finite resolution for practical devices. The successful application of our framework to this case improves the practical security of CV systems.

Here we will explain some details of our design principle for the discrete-distributed coherent states case. The three-mode entangled source model we use is not only simple-structure, but also highly effective.

A. Two-mode entangled source

Suppose the source states are n different coherent states $S_\rho = \{|\alpha_{B_0}^1\rangle, |\alpha_{B_0}^2\rangle, \dots, |\alpha_{B_0}^n\rangle\}$, and the three-mode entangled source is $|\psi_{ACB_0}\rangle$. From the discussion of section II. B we know that, the performance of a protocol is mainly decided by the structure of ρ_{CB_0} . Therefore, our design principle is to

let the correlation between modes C and B_0 as ‘high’ as possible, which from the covariance matrix pointview we want $|\langle \Delta \hat{x}_C \Delta \hat{x}_{B_0} \rangle|$ and $|\langle \Delta \hat{p}_C \Delta \hat{p}_{B_0} \rangle|$ to be as large as possible. We note that our design principle is only an example inspired by the experience, and it works well for the quadrature-amplitude modulation (QAM) case. Other design solutions for different modulation cases also worth further investigations.

Suppose the covariance matrix γ_{ACB_0} for $|\psi_{ACB_0}\rangle$ is of the standard form [31, 32], which means all $\langle \Delta \hat{x}_i \Delta \hat{p}_j \rangle = 0, \forall i, j$. This can be achieved in the QAM case.

We take x -quadrature as the example. Denote the mean and the variance of each sub-state ρ_C^i and $|\alpha_{B_0}^i\rangle$ as

$$\begin{aligned} \bar{x}_C^i &= \text{Tr}_C (\hat{x}_C \rho_C^i), V_{C,x}^i = \text{Tr}_C (\hat{x}_C^2 \rho_C^i) - (\bar{x}_C^i)^2, \\ \bar{x}_{B_0}^i &= \langle \alpha_{B_0}^i | \hat{x}_{B_0} | \alpha_{B_0}^i \rangle, V_{B_0,x}^i = 1. \end{aligned} \quad (15)$$

Then the overall mean values of modes C and B_0 are $\bar{x}_C = \sum_{i=1}^n p_i \bar{x}_C^i$, $\bar{x}_{B_0} = \sum_{i=1}^n p_i \bar{x}_{B_0}^i$, and the variances are

$$\begin{aligned} V_{C,x} &= \sum_{i=1}^n p_i V_{C,x}^i + \sum_{i=1}^n p_i (\bar{x}_C^i - \bar{x}_C)^2, \\ V_{B_0,x} &= 1 + \sum_{i=1}^n p_i (\bar{x}_{B_0}^i - \bar{x}_{B_0})^2. \end{aligned} \quad (16)$$

Now look at $|\langle \Delta \hat{x}_C \Delta \hat{x}_{B_0} \rangle|$, which is

$$\begin{aligned} |\langle \Delta \hat{x}_C \Delta \hat{x}_{B_0} \rangle| &= |\langle (\hat{x}_C - \bar{x}_C)(\hat{x}_{B_0} - \bar{x}_{B_0}) \rangle| \\ &= \left| \sum_{i=1}^n p_i \text{Tr}_{CB_0} [(\hat{x}_C - \bar{x}_C)(\hat{x}_{B_0} - \bar{x}_{B_0}) \rho_C^i \otimes \rho_{B_0}^i] \right| \\ &= \left| \sum_{i=1}^n p_i (\bar{x}_C^i - \bar{x}_C)(\bar{x}_{B_0}^i - \bar{x}_{B_0}) \right| \\ &\leq \sqrt{\left(\sum_{i=1}^n p_i (\bar{x}_C^i - \bar{x}_C)^2 \right) \left(\sum_{i=1}^n p_i (\bar{x}_{B_0}^i - \bar{x}_{B_0})^2 \right)} \\ &= \sqrt{\left(V_{C,x} - \sum_{i=1}^n p_i V_{C,x}^i \right) (V_{B_0,x} - 1)}. \end{aligned} \quad (17)$$

The inequality is due to the Cauchy-Schwarz inequality, in which the equality holds if and only if $\forall i \in [1, n], (\bar{x}_C^i - \bar{x}_C)/(\bar{x}_{B_0}^i - \bar{x}_{B_0}) \equiv t$, where t is non-zero. The uncertainty principle tells that for each sub-state, $V_{C,x}^i V_{B_0,x}^i \geq 1$. If we further assume that x and p are symmetric for each sub-state, then $V_{C,x}^i \geq 1$, and $\sum_{i=1}^n p_i V_{C,x}^i \geq 1$. Thus, to achieve the maximum $|\langle \Delta \hat{x}_C \Delta \hat{x}_{B_0} \rangle|$, we need $V_{C,x}^i = 1$. One can find that these two conditions can be both satisfied if each ρ_C^i is also a coherent state $|\alpha_C^i\rangle$, with the mean value linearly dependent on $|\alpha_{B_0}^i\rangle$, which is $\forall i \in [1, n], \alpha_C^i / \alpha_{B_0}^i = t$. This linear relationship can be got from a beamsplitter model, which is a coherent state $|\beta_D^i\rangle$ with $\beta_D^i = \sqrt{1+t^2} \alpha_{B_0}^i$ passes through a beamsplitter with transmittance $\eta_{BS} = 1/(1+t^2)$. This means Alice only needs to generate a two-mode entangled state $|\psi_{AD}\rangle = \sum_{i=1}^n \sqrt{p_i} |R_A^i\rangle |\beta_D^i\rangle$, and then let the mode D

pass through a beamsplitter, shown as Fig. 2 in the main context.

As for the design of $|\psi_{AD}\rangle$, first, we find a set of orthogonal states $\{|\theta_D^i\rangle = \sum_{j=0}^{\infty} c_{ij} |j\rangle\}$, which can diagonalize the mixed state ρ_D , such that

$$\rho_D = \sum_{i=1}^n p_i |\beta_D^i\rangle \langle \beta_D^i| = \sum_{i=1}^n v_i |\theta_D^i\rangle \langle \theta_D^i| \quad (18)$$

Then $|\psi_{AD}\rangle$ is defined as

$$|\psi_{AD}\rangle = \sum_{i=1}^n \sqrt{v_i} |\varphi_A^i\rangle |\theta_D^i\rangle, \quad (19)$$

where $|\varphi_A^i\rangle$ is related to $|\theta_D^i\rangle$ in such a way,

$$|\varphi_A^i\rangle = \sum_{j=0}^{\infty} (c_{ij})^* |j\rangle. \quad (20)$$

B. Quadrature-amplitude modulation (QAM)

We are especially interested in the QAM case, because it's a standard modulation format in the classical coherent communication. Systems running such a modulation format is naturally compatible with current industry chain of electro-optical devices.

In n -QAM ($n = L^2$, L is positive integer), coherent states are positioned at the cross points of equally-spaced L columns and L rows in the phase space (or classically called constellation map). Suppose the space between each column (or row) is $2r$, then the positions of n coherent states are

$$\{\forall \mu, v \in [1, L], \alpha_{\mu v} = (2\mu - 1 - L)r + i \cdot (2v - 1 - L)r\}$$

It can be verified that for this standard QAM format, the covariance matrix for $|\psi_{AD}\rangle$ is of the standard form,

$$\gamma_{AD} = \begin{pmatrix} V_A I & \phi_{AD} \sigma_Z \\ \phi_{AD} \sigma_Z & V_A I \end{pmatrix} \quad (21)$$

where $I = \begin{pmatrix} 1 & 0 \\ 0 & 1 \end{pmatrix}$, and $\sigma_Z = \begin{pmatrix} 1 & 0 \\ 0 & -1 \end{pmatrix}$. We know that $\phi_{AD} \leq \sqrt{V_A^2 - 1}$ due to the uncertainty principle, and the closer ϕ_{AD} approaches to $\sqrt{V_A^2 - 1}$, the better the protocol performance will be. Thus, for the n -QAM, we need to choose the proper sending probabilities $\{p_1, \dots, p_n\}$ and the space parameter r to make the ϕ_{AD} as large as possible. Since the different $\{p_1, \dots, p_n\}$ and r will result in different V_A , we introduce a dimensionless parameter $\eta_A = \phi_{AD}^2 / (V_A^2 - 1)$ to evaluate the closeness of ϕ_{AD} to $\sqrt{V_A^2 - 1}$ for the small V_A region.

Fully optimization of the probabilities $\{p_1, \dots, p_n\}$ is complicated. Here we let them follow a discrete Gaussian distribution: let $r_0 = 1$ (the unit is the square root of the shot noise unit (SNU)), then the probability $p(\alpha_{\mu v})$ of sending the state $|\alpha_{\mu v}\rangle$ is

$$p(\alpha_{\mu v}) \propto \exp \left[-|\alpha_{\mu v}(r = r_0)|^2 / (2V_G) \right]. \quad (22)$$

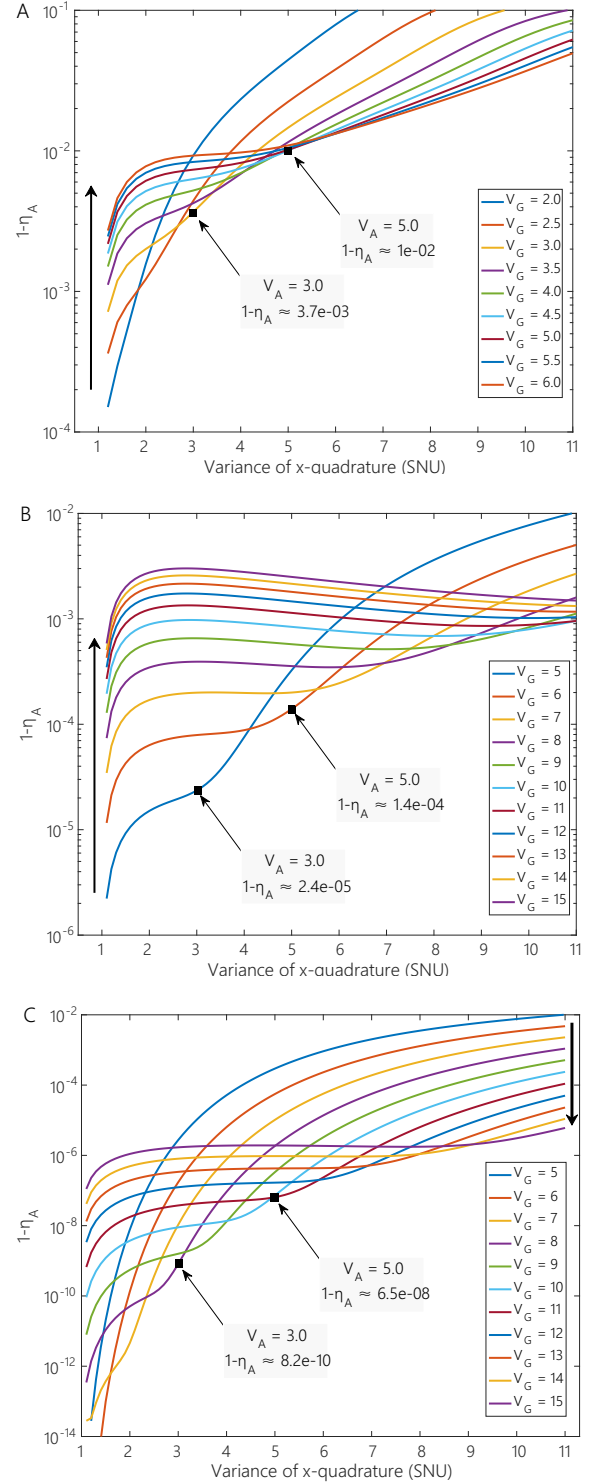


FIG. 5. $1 - \eta_A$ versus V_A . (A) 16-QAM case, curves following the direction of the arrow (left side bottom-up) correspond to the cases of $V_G = 2.0 \sim 6.0$. (B) 64-QAM case, curves following the direction of the arrow (left side bottom-up) correspond to the cases of $V_G = 5 \sim 15$. (C) 256-QAM case, curves following the direction of the arrow (right side top-down) correspond to the cases of $V_G = 5 \sim 15$. We mark the optimal V_G and the corresponding $1 - \eta_A$ for two different conditions $V_A = 3$ and $V_A = 5$.

This simplifies the probability distribution to only one parameter V_G .

We numerically calculate the η_A for 16-QAM, 64-QAM and 256-QAM, with different V_G and r , to find a relatively optimal combination of V_A and η_A . Generally speaking, for the small V_A region, the larger the V_A is, the worse the η_A is. Fig. 5 shows our simulation result. For 16-QAM (Fig. 5(A)), when $V_A = 3$, the optimal choice for V_G is $V_G = 3$, which corresponds to $\eta_A \approx 1 - 3.7 \times 10^{-3}$; when $V_A = 5$, the optimal choice for V_G is $V_G = 4.5$, which corresponds to $\eta_A \approx 1 - 1 \times 10^{-2}$. For 64-QAM (Fig. 5(B)), when $V_A = 3$, the optimal choice for V_G is $V_G = 5$, which corresponds to $\eta_A \approx 1 - 2.4 \times 10^{-5}$; and when $V_A = 5$, the optimal choice for V_G is $V_G = 6$, which corresponds to $\eta_A \approx 1 - 1.4 \times 10^{-4}$. For 256-QAM (Fig. 5(C)), when $V_A = 3$, the optimal choice for V_G is $V_G = 8$, which corresponds to $\eta_A \approx 1 - 8.2 \times 10^{-10}$; and when $V_A = 5$, the optimal choice for V_G is $V_G = 11$, which corresponds to $\eta_A \approx 1 - 6.5 \times 10^{-8}$.

From the η_A -pointview, 256-QAM is almost the ideal Gaussian case, and such a small deviation won't cause a large performance reduction. This is verified by the secret key rate simulation shown in the Fig. 3 of the main context.

In experiment, the two quadratures can be modulated separately, for instance using the QPSK modulator. Thus, for the L^2 -QAM, the resolution of the DAC device for the modulation of one quadrature is $res = \log_2 L$. Then for 16-QAM, $res = 2$, 64-QAM, $res = 3$, and for 256-QAM, $res = 4$. DAC devices with such resolutions are off-the-shell and cost-effective.

C. Techniques for the numerical calculation

Numerical calculation is needed in two parts, in which the first is the calculation of γ_A , γ_C and ϕ_{AC} , and the second is the searching process.

For the calculation of γ_A , γ_C and ϕ_{AC} , a simple way is to express every state, e.g. $|\alpha_{B_0}^i\rangle$, $|\theta_D^i\rangle$ and $|\phi_D^i\rangle$, in the Fock state basis, and then finish the calculation. One thing needs to be careful with is, to achieve high precision, the number of Fock state bases should be greatly larger than $\sqrt{V_A}$. For example, for $V_A = 10$, we choose first 200 Fock states to express a state. This numerical method fits well with the theoretical results for the 4-QAM case in [22].

For the searching process, although the three-mode entangled state model already has the least unknown parameters, the symmetry of the QAM case can further simplify it.

First, we define the standard form of the covariance matrix for the three-mode EB scheme for L^2 -QAM. After Bob sharing part of his measurement results, the sub covariance matrix γ_{CB} of modes C and B can be transformed to the standard form γ_{CB}^{std} [31, 32], which is

$$\gamma_{CB}^{std} = \begin{pmatrix} [(1 - \eta_{BS})(V_A - 1) + 1]I & \begin{pmatrix} \phi_x & 0 \\ 0 & \phi_p \end{pmatrix} \\ \begin{pmatrix} \phi_x & 0 \\ 0 & \phi_p \end{pmatrix} & V_B I \end{pmatrix}, \quad (23)$$

through two local unitary operators over modes C and B with corresponding symplectic matrices S_C and S_B . ϕ_x and ϕ_p may not be equal. Then one can find a unitary operator over mode A with the corresponding symplectic matrix S_A , such that $S_A \sigma_Z S_C^T = \sigma_Z$. Therefore, the covariance matrix γ_{ACB} can be 'standardized' by these three operators $S = S_A \oplus S_C \oplus S_B$:

$$\gamma_{ACB}^{std} = S \gamma_{ACB} S^T = \begin{pmatrix} V_A I & -\sqrt{(1 - \eta_{BS})\eta_A(V_A^2 - 1)}\sigma_Z & \kappa'_{AB} \\ -\sqrt{(1 - \eta_{BS})\eta_A(V_A^2 - 1)}\sigma_Z & [(1 - \eta_{BS})(V_A - 1) + 1]I & \begin{pmatrix} \phi_x & 0 \\ 0 & \phi_p \end{pmatrix} \\ \kappa'_{AB} & \begin{pmatrix} \phi_x & 0 \\ 0 & \phi_p \end{pmatrix} & V_B I \end{pmatrix} \quad (24)$$

where $\kappa'_{AB} = S_A \kappa_{AB} S_B^T = \begin{pmatrix} \kappa_{11} & \kappa_{12} \\ \kappa_{21} & \kappa_{22} \end{pmatrix}$ is still unknown.

For this standard form, it is found that, no matter Bob uses heterodyne or homodyne detection, the secret key rate for the case $\gamma_{ACB}^{std}(\kappa_{11}, \kappa_{12}, \kappa_{21}, \kappa_{22})$ (denote this state as $\rho_{ACB}^{(+)}$) and the case $\gamma_{ACB}^{std}(\kappa_{11}, -\kappa_{12}, -\kappa_{21}, \kappa_{22})$ (denote this state as $\rho_{ACB}^{(-)}$) are the same. If we further define a state as the equally mixture of the above two cases, $\rho_{mix} = (\rho_{ACB}^{(+)} + \rho_{ACB}^{(-)})/2$, then its covariance matrix will be $\gamma_{ACB}^{std}(\kappa_{11}, 0, 0, \kappa_{22})$. And from the sub-additivity of the secret key rate, we know $K(\rho_{mix}) \leq (K(\rho_{ACB}^{(+)} + K(\rho_{ACB}^{(-)}))/2 = K(\rho_{ACB}^{(+)}))$. Therefore, the lowest secret key rate case must happen at the condition $\kappa_{12} = \kappa_{21} =$

0. This further simplifies the searching process to two unknown parameters κ_{11} and κ_{22} .

When $\kappa_{12} = \kappa_{21} = 0$, it is found that the secret key rate is unchanged when $(\kappa_{11}, \kappa_{22}, \phi_x, \phi_p)$ becomes $(-\kappa_{22}, -\kappa_{11}, \phi_p, \phi_x)$. This means, if $\phi_x = \phi_p$, the lowest secret key rate happens at the condition $\kappa_{11} + \kappa_{22} = 0$, which further simplifies the searching process to only one unknown parameter κ_{11} .

Suppose $\Gamma = \gamma_{ACB}^{std} + i\Omega$, and $\Gamma_{i_1 j_2 \dots j_k}^{i_1 j_2 \dots j_k}$ represents the minor determinant of order k of Γ . The possible range for κ_{11} and κ_{22} , limited by the uncertainty principle, are $\kappa_{11} \in [\bar{\kappa}_{11} - R_x, \bar{\kappa}_{11} + R_x]$ and $\kappa_{22} \in [\bar{\kappa}_{22} - R_p, \bar{\kappa}_{22} + R_p]$, where

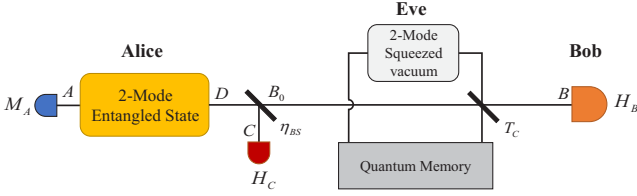


FIG. 6. **Schematic of the entangling cloner attack.** Eve generates a two-mode squeezed vacuum state, and send one mode to her quantum memory. She then interacts the other mode with mode B_0 using a beamsplitter (BS), whose transmittance equals to the channel transmittance T_C . She will send one mode after the BS to Bob, and keep the other mode in the quantum memory. After collecting enough many rounds, Eve will conduct the joint measurement on all states kept in her quantum memory.

$$\bar{\kappa}_{11} = -\phi_x \Gamma_{124}^{234} / \Gamma_{234}^{234}, \bar{\kappa}_{22} = -\phi_p \Gamma_{134}^{123} / \Gamma_{134}^{134}, \text{ and}$$

$$R_x = \left(V_B \Gamma_{1234}^{1234} / \Gamma_{234}^{234} - \phi_x^2 \left[\Gamma_{124}^{124} \Gamma_{234}^{234} - (\Gamma_{124}^{234})^2 \right] / (\Gamma_{234}^{234})^2 \right)^{1/2}$$

$$R_p = \left(V_B \Gamma_{1234}^{1234} / \Gamma_{134}^{134} - \phi_p^2 \left[\Gamma_{134}^{134} \Gamma_{123}^{123} - (\Gamma_{134}^{123})^2 \right] / (\Gamma_{134}^{134})^2 \right)^{1/2}$$

We note that, even if without these symmetry-induced simplifications, two facts indicate that the general linear searching algorithms also work effectively for the searching process: 1) the possible set S_κ is a connected set; 2) the sub-additivity of the secret key rate indicates that usually there is only one minimum point of the secret key rate.

D. Parameters for the numerical simulation

Here we explain the parameters used for the simulation in Fig. 3 of the main context. We consider the reverse reconciliation case, and assume that Bob uses homodyne detector. The reconciliation efficiency is assumed to be 0.95. From the

Fig. 5, we know that generally speaking the smaller the V_A is, the closer the η_A approaches to 1. However, if V_A is too small, its ability to tolerate the channel excess noise will decrease. Therefore, in the simulation, we choose $V_A = 3$ for 16-QAM, and $V_A = 5$ for both 64-QAM and 256-QAM. The corresponding η_A are $1 - 3.7 \times 10^{-3}$, $1 - 1.4 \times 10^{-4}$ and $\eta_A = 1 - 6.5 \times 10^{-8}$, respectively.

To simulate the terms in the sub covariance matrix γ_{CB} , we assume the channel eavesdropping model is the entangling-cloner attack [23], which is commonly used in the performance simulation of one-way CV protocols. We note that the entangling-cloner attack may not be the optimal attack for QAM case. The reason we still choose it for the performance simulation is the channel usually behaves like this way in common experiments. The schematics of this attack is shown in Fig. 6. Eve generates a two-mode squeezed vacuum state with variance $V_E = (1 + T_C \epsilon_C) / (1 - T_C)$, where ϵ_C is the channel excess noise and T_C is the channel transmittance. She first sends one mode to her quantum memory, then interacts the other mode with mode B_0 using a beamsplitter (BS), whose transmittance equals to T_C . After this, she will send one mode after the BS to Bob, and keep the other mode in the quantum memory. After collecting enough many rounds, Eve will conduct a joint measurement on all states in her quantum memory.

For another parameter η_{BS} , which is the transmittance of the BS used to split the mode D into modes C and B_0 . We choose it to be $\eta_{BS} = 0.9$. This means in our simulation, if $V_A = 3$, then the variance of ρ_{B_0} is 2.8, and if $V_A = 5$, then the variance of ρ_{B_0} is 4.6. Therefore, to compare 256-QAM with ideal Gaussian case, we keep the variance of the state incident into the channel being the same, which means the variance for the ideal Gaussian case is also set to 4.6. Additionally, we know that different η_{BS} correspond to different entangled source, which will show different performances. And the higher the η_{BS} is, the smaller the V_A is. Thus, roughly speaking, higher η_{BS} means better the performance. This parameter can also be optimized according to different channel conditions, if required.

-
- [1] C. H. Bennett and G. Brassard, *Quantum cryptography: Public key distribution and coin tossing*, in Proc. IEEE Int. Conf. on Computers, Systems and Signal Processing 175–179 (IEEE Press, 1984).
 - [2] N. Gisin, G. Ribordy, W. Tittel, and H. Zbinden, *Quantum cryptography*, Rev. Mod. Phys. **74**, 145 (2002).
 - [3] V. Scarani, H. Bechmann-Pasquinucci, N. J. Cerf, *et al.*, *The security of practical quantum key distribution*, Rev. Mod. Phys. **81**, 1301 (2009).
 - [4] H. K. Lo, M. Curty, K. Tamaki, *Nature Photon.*, *Secure quantum key distribution*, **8**, 595–604 (2014).
 - [5] T. C. Ralph, *Continuous variable quantum cryptography*, Phys. Rev. A **61**, 010303 (1999).
 - [6] F. Grosshans and P. Grangier, *Continuous Variable Quantum Cryptography Using Coherent States*, Phys. Rev. Lett. **88**, 057902 (2002).
 - [7] C. Weedbrook, A. M. Lance, W. P. Bowen, *et al.*, *Quantum Cryptography Without Switching*, Phys. Rev. Lett. **93**, 170504 (2004).
 - [8] R. García-Patrón and N. J. Cerf, *Continuous-variable quantum key distribution protocols over noisy channels*, Phys. Rev. Lett. **102**, 130501 (2009).
 - [9] S. L. Braunstein, P. van Loock, *Rev. Mod. Phys.* *Quantum information with continuous variables*, **77**, 513 (2005).
 - [10] C. Weedbrook, S. Pirandola, R. García-Patrón *et al.*, *Gaussian quantum information*, Rev. Mod. Phys. **84**, 621 (2012).
 - [11] E. Diamanti and A. Leverrier, *Distributing Secret Keys with Quantum Continuous Variables: Principle, Security and Implementations*, Entropy **17**, 6072–6092 (2015).
 - [12] F. Grosshans, G. Van Assche, J. Wenger, *et al.*, *Quantum key distribution using gaussian-modulated coherent states*, Nature **421**, 238 (2003).
 - [13] S. Pirandola, S. Mancini, S. Lloyd, and S. L. Braunstein, *Continuous-variable quantum cryptography using two-way*

- quantum communication*, Nature Phys., **4**, 726–730 (2008).
- [14] M. Navascués, F. Grosshans, and A. Acín, *Optimality of Gaussian attacks in continuous-variable quantum cryptography*, Phys. Rev. Lett. **97**, 190502 (2006).
 - [15] R. García-Patrón and N. J. Cerf, *Unconditional optimality of Gaussian attacks against continuous-variable quantum key distribution*, Phys. Rev. Lett. **97**, 190503 (2006).
 - [16] F. Furrer, T. Franz, M. Berta, *et al.*, *Continuous variable quantum key distribution: finite-key analysis of composable security against coherent attacks*, Phys. Rev. Lett. **109**, 100502 (2012).
 - [17] A. Leverrier, *Composable security proof for continuous-variable quantum key distribution with coherent states*, Phys. Rev. Lett. **114**, 070501 (2015).
 - [18] A. Leverrier, *Security of Continuous-Variable Quantum Key Distribution via a Gaussian de Finetti Reduction*, Phys. Rev. Lett. **118**, 200501 (2017).
 - [19] P. Jouguet, S. Kunz-Jacques, E. Diamanti, and A. Leverrier, *Analysis of imperfections in practical continuous-variable quantum key distribution*, Phys. Rev. A **86**, 032309 (2012).
 - [20] Y.-B. Zhao, M. Heid, J. Rigas, and N. Lütkenhaus, *Asymptotic security of binary modulated continuous-variable quantum key distribution under collective attacks*, Phys. Rev. A, **79**, 012307 (2009).
 - [21] K. Brádler, C. Weedbrook, *Security proof of continuous-variable quantum key distribution using three coherent states*, Phys. Rev. A **97**, 022310 (2018).
 - [22] A. Leverrier, and P. Grangier, *Unconditional security proof of long-distance continuous-variable quantum key distribution with discrete modulation*, Phys. Rev. Lett. **102**, 180504 (2009).
 - [23] F. Grosshans, N. J. Cerf, J. Wenger, *Virtual entanglement and reconciliation protocols for quantum cryptography with continuous variables*, *et al.*, Quantum Inf. Comput. **3**, 535–552 (2003).
 - [24] C. H. Bennett, G. Brassard, C. Crépeau, *et al.*, *Generalized privacy amplification*, IEEE Trans. Inf. Theory, **41**, 1915–1923 (1995).
 - [25] R. Renner, and R. König, *Universally composable privacy amplification against quantum adversaries*, Theory of Cryptography Conference, Springer Berlin Heidelberg, 407–425 (2005).
 - [26] I. Devetak, and A. Winter, *Distillation of secret key and entanglement from quantum states*, Proc. Roy. Soc. A **461**, 207 (2005).
 - [27] A. S. Holevo, *Bounds for the Quantity of Information Transmitted by a Quantum Communication Channel*, Probl. Inf. Transm. **9**, 177 (1973).
 - [28] M. M. Wolf, G. Giedke, and J. I. Cirac, *Extremality of Gaussian quantum states*, Phys. Rev. Lett. **96**, 080502 (2006).
 - [29] P. Jouguet, S. Kunz-Jacques, A. Leverrier, *et al.*, *Experimental demonstration of long-distance continuous-variable quantum key distribution*, Nature Photon., **7**, 378–381 (2013).
 - [30] V. Bargmann, P. Butera, L. Girardello, and J. R. Klauder, *On the completeness of the coherent states*, Rep. Math. Phys. **2**, 221–228 (1971).
 - [31] L.-M. Duan, G. Giedke, J. I. Cirac, and P. Zoller, *Inseparability criterion for continuous variable systems*, Phys. Rev. Lett. **84**, 2722 (2000).
 - [32] R. Simon, *Peres-Horodecki separability criterion for continuous variable systems*, Phys. Rev. Lett. **84**, 2726 (2000).